MAGNETIC RESONANCE IN CHEMISTRY, VOL. 35, 743–751 (1997)

Investigation of the Paramagnetic Domain of Putidaredoxin by Nitrogen-15 NMR Spectroscopy

Bruce Coxon,* Nese Sari, Marcia J. Holden and Vincent L. Vilker
Biotechnology Division, National Institute of Standards and Technology, Gaithersburg, Maryland 20899, USA

The oxidized forms of the redox proteins putidaredoxin and putidaredoxin-^{15}N were prepared by insertion of suitable plasmids into *E. coli* and the structures of the proteins were studied by homo- and heteronuclear ^{1}H and ^{15}N NMR methods, including identification of ^{15}N resonance types by one- and two-dimensional DEPT spectrum editing and measurements of ^{15}N chemical shifts, coupling constants, nuclear Overhauser effects and spin–lattice relaxation times. Direct detection of ^{15}N NMR spectra revealed a number of ^{15}N resonances that have not been found in previous ^{1}H detected NMR studies. These resonances include a set of 16 paramagnetically broadened signals from ^{15}N nuclei that are structurally close to the iron–sulfur cluster of the protein, proline backbone ^{15}N resonances and ^{15}N signals from the side-chains of glutamine and lysine residues. Reduced distances between certain paramagnetically affected ^{15}N nuclei and the center of the iron–sulfur cluster were calculated from the ^{15}N spin–lattice relaxation times, based on the assumption of a dominant electron–nuclear dipole–dipole relaxation mechanism. Ranked by size, these distances agree with those computed from coordinates of a published structure of putidaredoxin determined by ^{1}H NMR and analogy with an *Anabaena* ferredoxin. © **1997 John Wiley & Sons, Ltd.**

Magn. Reson. Chem. **35**, 743–751 (1997) No. of Figures: 5 No. of Tables: 3 No. of References: 52

Keywords: ^{15}N NMR; ^{1}H NMR; paramagnetic proteins; putidaredoxin; ^{15}N T_1 values; iron–sulfur cluster; reduced distances

Received 3 February 1997; revised 2 June 1997; accepted 4 June 1997

INTRODUCTION

Putidaredoxin is a paramagnetic, 11.6 kDa, 106 residue protein that occurs naturally in the soil bacterium *Pseudomonas putida*.[1] We are interested in the structure and electron transport properties of putidaredoxin, cytochrome $P450_{cam}$ and other redox proteins, from the point of view of their development as biocatalysts for the hydroxylation of hydrocarbons. These oxygenase enzymes have considerable potential for the industrial production of high-value chemicals in which hydroxyl groups are introduced into hydrocarbons in a regio- and stereo-specifically controlled manner. An improved understanding of the electron transport mechanisms in these proteins could lead to enhanced yields in hydrocarbon oxygenation, which are currently low. A structure-based model for putidaredoxin–cytochrome $P450_{cam}$ interactions has been proposed.[2]

Putidaredoxin occurs in both oxidized (Pdx) and reduced forms, which contain different oxidation states Fe^{3+}–Fe^{3+} and Fe^{3+}–Fe^{2+} in the Fe_2S_2 cluster.[3] Both forms of Pdx and some diamagnetic metal analogs have been studied extensively by ^{1}H detected, homo- and heteronuclear NMR methods.[3–9] These analyses of the ^{1}H NOE data of Pdx have yielded a globular structure containing three α-helices, two β-sheets and two β-turns.[5] However, of the 106 amino acid residues in Pdx, about 20 are not well characterized by proton NMR, owing to a paramagnetic broadening that is worse than that in many metalloproteins.[10–14] So far, the very broad and overlapped, paramagnetically shifted resonances in the 23–42 ppm region of the ^{1}H NMR spectrum of Pdx (Ref. 3 and this work) have not been structurally useful. As a result, the existing NMR-derived structure of Pdx may be uncertain within about 8 Å of the Fe_2S_2 cluster.[6] The modeling of this cluster and its environment that was required to complete the structural analysis[6] of Pdx by ^{1}H NMR was of necessity based on geometry that had been established for the related *Anabaena* ferredoxin by x-ray crystal structure analysis.[15] The degree of spectral broadening depends on the strength of the field (Fermi contact and/or dipole–dipole) exerted by the metal at the position of the resonant nucleus and on the rate by which this interaction is modulated.[16]

An alternative approach to structure near the iron–sulfur cluster might involve ^{15}N detected NMR. The rationale for this is (a) the linewidth ($\Delta\nu_{1/2}$) is proportional to the transverse relaxation rate (T_2^{-1}) according to $T_2^{-1} = \pi\Delta\nu_{1/2}$, (b) the transverse relaxation rate is proportional[10] to the square of the magnetogyric ratio (γ_N^2):

$$T_2^{-1} = \frac{1}{15}\left(\frac{\mu_0}{4\pi}\right)^2 \frac{\gamma_N^2 g_e^2 \mu_B^2 S(S+1)}{r^6} \times \left[4\tau_c + \frac{\tau_c}{1+(\omega_I-\omega_S)^2\tau_c^2} + \frac{3\tau_c}{1+\omega_I^2\tau_c^2} + \frac{6\tau_c}{1+(\omega_I+\omega_S)^2\tau_c^2} + \frac{6\tau_c}{1+\omega_S^2\tau_c^2}\right] \quad (1)$$

* *Correspondence to*: B. Coxon. E-mail bruce.coxon@nist.gov

 CCC 0749–1581/97/110743–09 $17.50

for the dominating electron → nuclear dipole–dipole relaxation in the vicinity of the paramagnetic center and (c) ^{15}N NMR linewidths may be expected[17] to be up to 100 times smaller than the linewidths of protons near the paramagnetic cluster, since $\gamma_{N\text{-}15}$ is about 10 times smaller than γ_H. We have; therefore, investigated the structure of Pdx by directly detected ^{15}N NMR. The potential of this method has been demonstrated previously for other ferredoxins, particularly those from *Anabaena*.[17–20]

EXPERIMENTAL*

Expression and purification of Pdx-^{15}N

E. coli BL21 (DE3) were transformed with the plasmid vector PRE1 containing the gene for Pdx under the control of the λP_L promoter.[21] The gene for Pdx, originally from the plasmid PIBI25, was mutagenized using a site-directed mutagenesis protocol (Clonetech Laboratories) to introduce an *Nde*1 restriction site at the initiation codon for the gene. The gene was cut out of PIBI25 with *Nde*1 and *Sma*I and inserted into PRE1 cut with the same enzymes. *E. coli* BL21 (DE3) was transformed with PRE1/Pd1 and PRK248. These cells were subsequently transformed with a second plasmid, PRK248, which contained the gene for the temperature sensitive C1587 λ repressor.[22] The cells were grown initially on Terrific broth (a rich, undefined medium[23]) at 32 °C, a temperature at which there was no expression of Pdx; they were then harvested in the mid-logarithmic phase of growth, washed and transferred to a defined medium containing $^{15}NH_4Cl$ as the sole nitrogen source. Cell growth was continued at 39 °C (a permissive temperature for expression). After 5 h, the cells were harvested, lysed and purified by a two-step, chromatographic protocol[24] from the 29 000 *g* supernatant. In the first step, a DEAE-Sepharose column was used and Pdx-^{15}N was eluted with a gradient of KCl. Following concentration by ultrafiltration, the protein was chromatographed on a gel filtration column. The activity of the Pdx was then assayed and its purity verified by 2D gel electrophoresis. Electrospray mass spectrometry indicated that the ^{15}N enrichment of the protein was 90%. The purified Pdx-^{15}N was stored in 50 mmol l^{-1} MOPS–TRIS/100 mmol l^{-1} KC1 buffer at pH 7.4 and −80 °C until used. Aliquots of Pdx solution were pooled and concentrated by ultrafiltration using Amicon Centriprep centrifugal concentrators with YM10 filters. Phosphate buffer (10 mmol l^{-1}, pH 7.4) containing 0.25 mmol l^{-1} dithiothreitol was substituted for the storage buffer by sequential dilution and reconcentration until the MOPS concentration had been diminished to <0.5 mmol l^{-1}. The protein preparation was then purged with argon and checked for integrity and activity. The chemical purity of the protein was assessed by 1D and 2D ^1H NMR spectroscopy, particularly with respect to the presence of buffer residues, or such other contaminants as glycerol. The latter contaminant was eliminated by pre-washing the YM10 membrane filters with water.

* Certain commercial equipment, instruments or materials are identified in this paper to specify adequately the experimental procedure. Such identification does not imply recommendation by the National Institute of Standards and Technology, nor does it imply that the materials are necessarily the best available for the purpose.

NMR spectroscopy

^1H detected NMR spectra were measured mostly at 500 MHz and at 290 K by means of a Bruker AMX-500 spectrometer equipped with a 5 mm inverse triple resonance probe. The solutions (0.5 ml) contained 7 mmol l^{-1} Pdx or Pdx-^{15}N in 9:1 (v/v) H_2O–D_2O. The water signal was used as a secondary, internal ^1H chemical shift reference, and was set to 4.8493 δ, based on sodium 4,4-dimethyl-4-silapentanoate-2,2,3,3-d_4 (TSP) = 0. ^{15}N chemical shifts (δ_N) are reported with respect to external anhydrous liquid ammonia and were measured by use of an external capillary of saturated aqueous $^{15}NH_4^{15}NO_3$ solution as a secondary reference, for which the $^{15}NH_4$ resonance was set to 20.68 ppm. Data sets consisting of 4096 (F_2) × 512 (F_1) points zero-filled to either 1024 or 4096 points in the F_1 dimension were used for ^1H detected 2D NMR experiments, all in the TPPI mode.[25] Homonuclear 2D DQF-COSY,[26–28] NOESY,[29,30] ROESY[31,32] and TOCSY[33,34] experiments were conducted by using standard Bruker pulse programs with water presaturation, together with a ^1H 90° pulse width of 10.1 μs and a spectral width of 8.33 kHz in each dimension. Mixing times of 100, 70 and 60 ms were used for the NOESY, ROESY and TOCSY experiments, respectively.

^1H detected ^1H–^{15}N chemical shift correlations were performed by means of 2D HSQC[35] and HMQC[36] experiments, with ^1H and ^{15}N 90° pulses of 9.6 and 35.0 μs, respectively, and GARP decoupling[37] of ^{15}N during acquisition. Water presaturation was used for 2D HSQC, together with spectral widths of 11.4 and 10.0 kHz in the F_1 and F_2 dimensions, respectively. 2D HMQC spectra were acquired without water presaturation, with spectral widths of 3.55 and 5.05 kHz in the F_1 and F_2 dimensions, respectively.

^{15}N NMR measurements in the normal (direct) mode were performed at 40.55 MHz and 290 K by use of a Bruker WM-400 spectrometer equipped with a selective 10 mm ^{15}N probe, a selective ^{15}N preamplifier, an Aspect 3000 computer, an array processor, digital frequency generation and a process controller. All ^{15}N NMR spectra were acquired from 1.2–2.0 ml volumes of 7 mmol l^{-1} solutions of Pdx-^{15}N in 9:1 (v/v) H_2O–D_2O. The 1D ^{15}N NMR spectra were acquired by using 8192 or 16 384 data points, zero-filled in the latter case to 32 768 points, a spectral width of 12.2 kHz, a ^{15}N 90° pulse width of 23 or 64 μs and a ^1H 90° pulse width of 47 μs, where relevant. These spectra were acquired in seven modes: (a) ^1H decoupled with NOE, using continuous WALTZ-16 composite pulse decoupling[38] (CPD), (b) ^1H decoupled without NOE, using inverse gated CPD, (c) ^1H coupled with NOE,

using gated CPD, (d) ^{1}H coupled without NOE (CPD off), (e) DEPT45, (f) DEPT90 and (g) DEPT135.[39–41] ^{15}NH subspectra were obtained from the DEPT90 data, whereas $^{15}NH_2$ subspectra were computed as DEPT135-DEPT45.

^{15}N T_1 values were measured by 1D inversion–recovery[42] using 20 delay times ranging from 0.001 to 6 s, with nine cycles through the set of delay times. Measurements of paramagnetically broadened signals were performed by using six to eight delay times in the range 0.005–0.5 s, with four cycles through the delay times, and up to 16 000 scans per spectrum. Relaxation data were analysed with the Bruker DISR94 program, version 940 401.0, running on the Bruker Aspect 3000 computer. A three-parameter exponential fit was used to compute the T_1 data.

A 2D ^{15}N–^{1}H chemical shift correlation was implemented by HETCOR with BIRD decoupling of vicinal ^{1}H–^{1}H couplings in the F_1 dimension,[43] WALTZ-16 ^{1}H decoupling in the F_2 dimension, 2048 (F_2) × 200 or 320 (F_1) point data sets zero-filled to 512 points in the F_1 dimension, spectral widths of 3.70 and 9.26 kHz in the F_1 and F_2 dimensions, respectively and 256 or 320 scans per spectrum. By the use of similar parameters, a 2D ^{15}NH only subspectrum was obtained by 2D DEPT90 HETCOR ^{15}N–^{1}H chemical shift correlation spectrum editing.[40,41,44–46]

Most NMR data were processed with a Silicon Graphics Indigo computer, using the Bruker UXNMR and AURELIA programs, versions 941 001.1 and 2.0, respectively. Molecular modeling was conducted with the HYPERCHEM program, version 4.0 (Hypercube, Waterloo, Ontario, Canada).

RESULTS AND DISCUSSION

^{1}H detected NMR spectra of Pdx and Pdx-^{15}N

The identity of our samples of Pdx with earlier preparations[3–7,9] was confirmed by comparison of 2D DQF-COSY, NOESY, ROESY and TOCSY NMR data with those reported previously.[5] The 2D HSQC and HMQC NMR spectra of our preparation of Pdx-^{15}N measured at 500 MHz/50.6 MHz were very similar to each other and to a published 2D HSQC spectrum,[9] with the exception of differences due to spectral folding in the latter spectrum. Since Lyons *et al.*[9] were able to use 3D NMR methods for verification of many of the ^{15}N NMR assignments of ^{15}N nuclei that show proton connectivities, we accept their assignments, and have used them in the analysis of our ^{15}N relaxation data. However, our 2D HMQC spectrum of Pdx-^{15}N showed four cross peaks that do not appear to have been detected before. We assigned one cross peak at δ_N/δ_H 120.7/8.18 to the backbone NH group of D95 on the basis of agreement with the published chemical shift δ_H 8.17 of this NH proton.[5] The ^{15}N chemical shift of residue D95 was also detected in the directly observed ^{15}N NMR spectrum of Pdx-^{15}N. Two other HMQC cross peaks at δ_N/δ_H 121.5/9.256 and 122.0/7.877 may represent the backbone NH groups of Q25 and H49, which are absent from previous data sets.[9] A fourth HMQC cross peak is discussed later in the section on ^{15}N NOEs.

^{15}N detected NMR spectra of Pdx-^{15}N: ^{15}N chemical shifts

Direct detection of the 1D ^{15}N NMR spectra of Pdx-^{15}N was performed without polarization transfer in four data acquisition modes: (a) ^{1}H decoupled with NOE, (b) ^{1}H decoupled without NOE, (c) ^{1}H coupled with NOE and (d) ^{1}H coupled without NOE (see Figs 1 and 2). These spectra display a number of ^{15}N resonances that have not been observed in previous studies by ^{1}H detection, including four proline resonances, three lysine $N_\zeta H_2$ signals at high field and at least 16 broader resonances in the 104–310 ppm region that may be characterized as paramagnetically broadened and/or shifted signals (see Fig. 3). The lysine N_ζ resonances are not observed in ^{1}H detected experiments or in normal mode ^{15}N–^{1}H chemical shift correlation experiments, because of rapid exchange of the $N_\zeta H_2$ protons.

^{1}H-coupled ^{15}N NMR spectra

The observation of a doublet ($^{1}J_{NH}$ 96.9 Hz) at 167.8 ppm (see Fig. 2) confirms its assignment[9] as $N_{\delta 1}H$ of an imidazole ring (H49). In contrast, the $N_{\varepsilon 2}$ resonance at 244.7 ppm remains as a singlet under ^{1}H coupled conditions (see Fig. 2), which is consistent with assignment[9] of this resonance as the tertiary, unprotonated ring nitrogen $N_{\varepsilon 2}$ in H49. Overlapped doublets ($^{1}J_{NH}$ 92.4 and 93.3 Hz) at 84.6 and 83.5 ppm and triplets at *ca.* 70 ppm indicate the presence of the arginine $N_\varepsilon H$ and $N_\eta H_2$ groups, respectively. In the ^{1}H coupled ^{15}N NMR spectra, two of the lysine $N_\zeta H_2$ signals appear as a broad singlet and one other as a sharp singlet, indicating that the protons in these groups are in intermediate and rapid rates of exchange, respectively.

1D and 2D DEPT ^{15}N NMR

As expected, the 1D DEPT45 ^{15}N NMR spectrum of Pdx-^{15}N [Fig. 4(a)] displays all resonances with positive phase, whereas the corresponding DEPT135 spectrum [Fig. 4(c)] shows some resonances with negative phase that are assigned as $^{15}NH_2$ groups. A ^{15}NH only spectrum [Fig. 4(b)] was obtained by use of the 1D DEPT90 sequence. It was found that 1D spectrum editing using the DEPT135–DEPT45 combination yielded a $^{15}NH_2$ only spectrum [Fig. 4(d)], which shows five resonances of varying intensity in the NH backbone region, that were assigned to the asparagine and glutamine side-chain $^{15}NH_2$ groups indicated in Fig. 4(d), on the basis of their proton multiplicities and ^{15}N chemical shifts. The strong intensity of the ^{15}N peak at 112.8 ppm suggests the possibility that this peak may contain one or two resonances in addition to the N_ε signal of

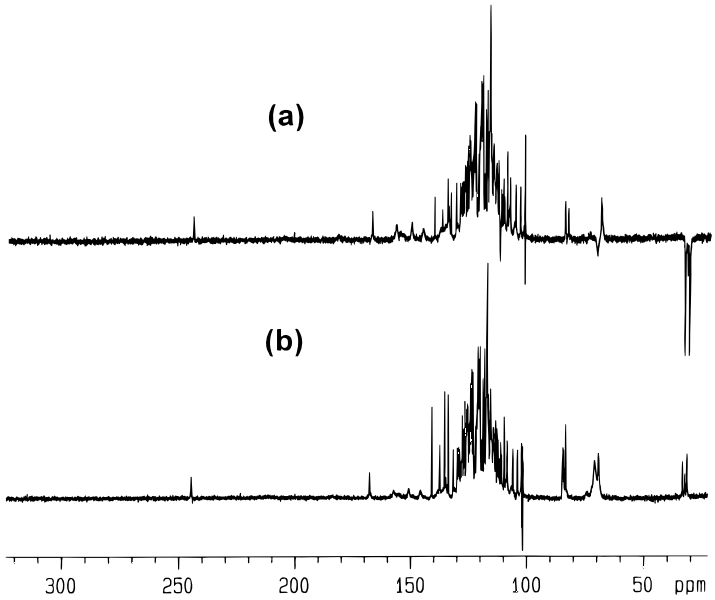

Figure 1. ^{15}N NMR spectra of a 7 mmol l^{-1} solution of Pdx-^{15}N in 9:1 (v/v) H_2O–D_2O measured at 40.55 MHz and 290 K: (a) ^{1}H decoupled with NOE; (b) ^{1}H decoupled without NOE. In (a), the strong negative NOEs of the lysine side-chain ^{15}N nuclei are noteworthy. A spectrometer artifact is present at *ca*. 102 ppm.

Q105 (see the next section on NOEs). No $^{15}NH_3$ groups were detected by either the 1D or 2D DEPT ^{15}N NMR techniques, evidently because rapid proton exchange does not allow evolution of $^1J_{NH}$.

A complete 2D ^{15}N–H chemical shift correlation spectrum [Fig. 5(a)] was obtained in the direct mode by non-DEPT HETCOR and the corresponding ^{15}NH only subspectrum [Fig. 5(b)] by 2D DEPT90 spectrum editing. These spectra provided alternative renditions to 2D HMQC and HSQC, but had very similar characteristics, i.e. no correlation cross peaks were detected for paramagnetically broadened ^{15}N resonances. One unique, unbroadened cross peak was detected in the 2D ^{15}N–^{1}H HETCOR spectrum at δ_N/δ_H 125.0/14.0 which, because of its low-field ^{1}H shift, may possibly originate from the backbone NH group of a residue in the paramagnetic zone, for example, the previously unassigned M24 or H49 residues.

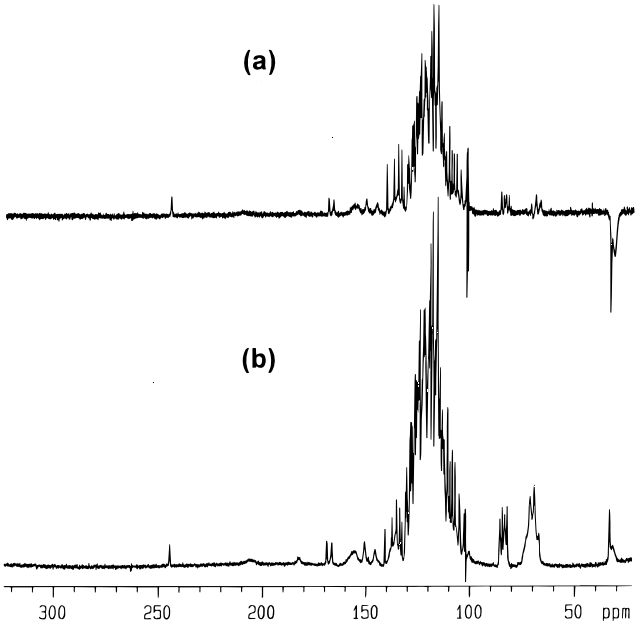

Figure 2. ^{15}N NMR spectra of Pdx-^{15}N measured at 40.55 MHz and 290 K: (a) ^{1}H coupled with NOE; (b) ^{1}H coupled without NOE. Comparison of these spectra with Fig. 1 reveals several one-bond ^{15}NH coupling constants. A spectrometer artifact is present at *ca*. 102 ppm.

^{15}N nuclear Overhauser effects

The lysine $N_\zeta H_2$ signals display strong negative NOEs [see Figs 1(a) and 2(a)] that are consistent with short correlation times and high mobility of these side-chain nitrogen atoms. Weaker negative NOEs are shown by the arginine $N_\eta H_2$ resonances at 71.1 ppm and by another ^{15}N resonance at 112.8 ppm. The latter resonance was also detected in the 2D HMQC spectrum of Pdx-^{15}N as a doublet of cross peaks at δ_N/δ_H 112.8/6.755 and 112.8/7.305. For several reasons, this resonance was assigned to the side-chain $N_\varepsilon H_2$ of Q105: (a) the multiplicity in the HMQC spectrum, (b) the $^{15}NH_2$ multiplicity indicated by the DEPT spectrum editing discussed before, (c) the negative NOE and (d) the relatively long ^{15}N T_1 of 0.3 s, are all consistent with assignment to a mobile, side-chain NH_2 group close to the C-terminus of the protein.

Comparison of the proton decoupled ^{15}N spectra obtained with and without NOE [see Fig. 1(a) and (b)] indicates that in the spectrum with NOE, the intensities of the (positive) proline ^{15}N signals are diminished by partial negative NOE contributions of < -1, which result, presumably, from some dipolar relaxation by

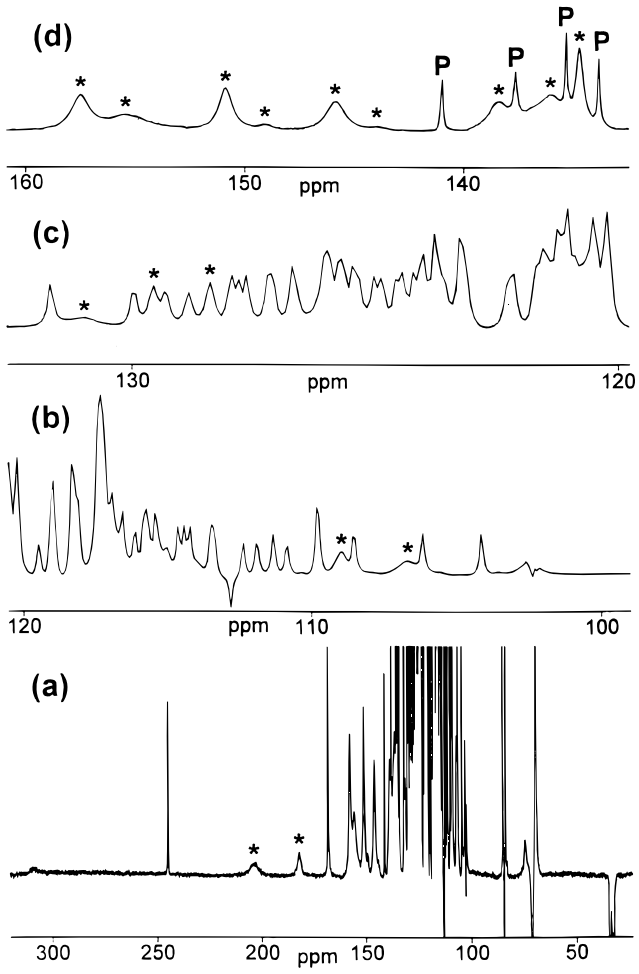

Figure 3. ^{15}N NMR spectra of Pdx-^{15}N measured at 40.55 MHz and 290 K under rapid pulsing conditions (acquisition time 0.34 s, 178 402 scans). The paramagnetically broadened resonances are identified by asterisks in the full spectrum (a) and in the expansions (b–d). In expansion (d), the proline resonances are identified by P. Spectral artifacts are present at *ca*. 102 and 309 ppm and the signals of ^{15}N nuclei having longer T_1 values are partially suppressed.

protons that are two bonds distant. All of the backbone amide ^{15}NH signals are positive, which implies longer correlation times and less mobility.

^{15}N relaxation times

^{15}N T_1 values of selected residues are given in Table 1. The backbone amide ^{15}NH values are in the range 0.33–0.46 s and are consistent with low mobility. Similar values are shown by the arginine $N_\eta H_2$ and asparagine $N_\delta H_2$ nitrogen nuclei, which, although more mobile, show short T_1 values due to relaxation contributions from two attached protons. Two of the lysine sidechain nitrogens show longer T_1 values (1.73 and 1.81 s), whereas one is shorter (0.32 s). Molecular modeling of the NMR determined structure[6] of Pdx indicates that all three lysine residues are on the surface of the protein and hence may have comparable exposure to solvent. The short T_1 (0.32 s) may possibly be assignable to K2 on the basis that a larger solvation shell near the N-terminus would be expected to increase the correlation time of the K2 residue. The latter residue and its immediate neighbors S1 and V3 contain a total of three solvatable sidechain groups (OH and $N_\alpha H_3^+$ in S1 and $N_\zeta H_3^+$ in K2), whereas the triad sequences L78–K79–P80 and D58–K59–V60 afford only one and two solvatable side-chain groups, respectively. The proline ^{15}N T_1s are longer (1.68–2.02 s) owing to the absence of dipolar relaxation by directly attached protons.

Calculation of distances of ^{15}N nuclei from the paramagnetic cluster

The distances of paramagnetically affected ^{15}N nuclei from the iron–sulfur cluster are related to their spin–lattice relaxation times by the equation

$$T_1^{-1} = \frac{4}{3}\left(\frac{\mu_0}{4\pi}\right)^2 \frac{\gamma_N^2 g_e^2 \mu_B^2 S(S+1)}{d_r^6}\,\tau_c \qquad (2)$$

given the assumption of a dominating electron → nuclear dipole–dipole relaxation mechanism.[17]

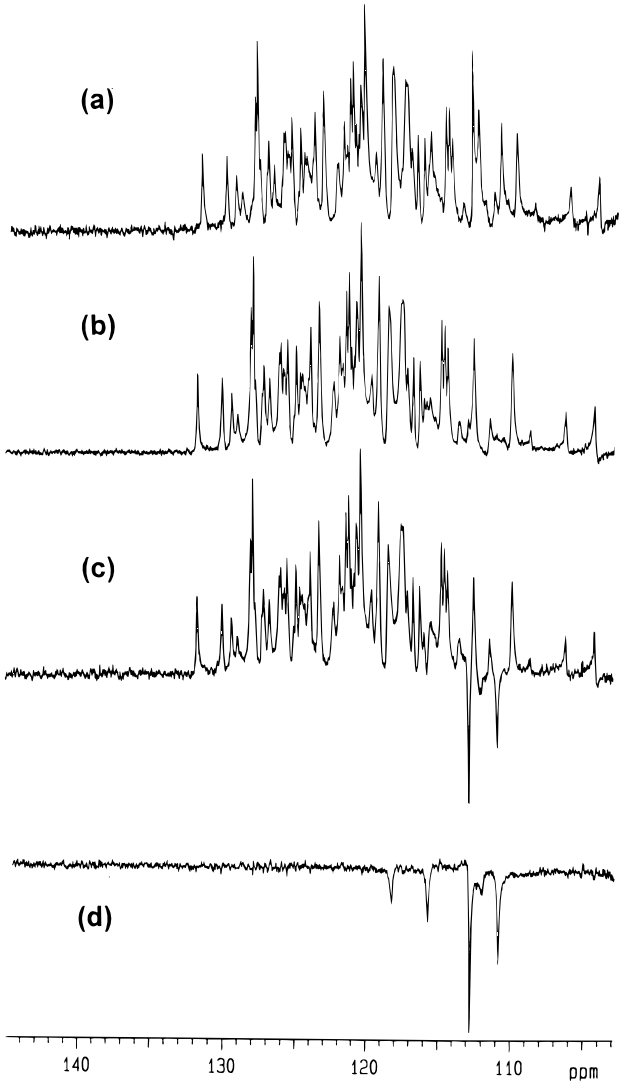

Figure 4. ^{15}N DEPT NMR spectra of Pdx-^{15}N at 40.55 MHz and 290 K: (a) DEPT45; (b) DEPT90 (^{15}NH subspectrum); (c) DEPT135; and (d) $^{15}NH_2$ subspectrum generated from DEPT135-DEPT45, showing the $^{15}N_\delta$ signals of several asparagine residues and the $^{15}N_\varepsilon$ signal of the glutamine residue Q105. The $^{15}N_\varepsilon$ signal of Q25 at 103.5 ppm[9] is obscured by a spectrometer artifact at *ca.* 102 ppm.

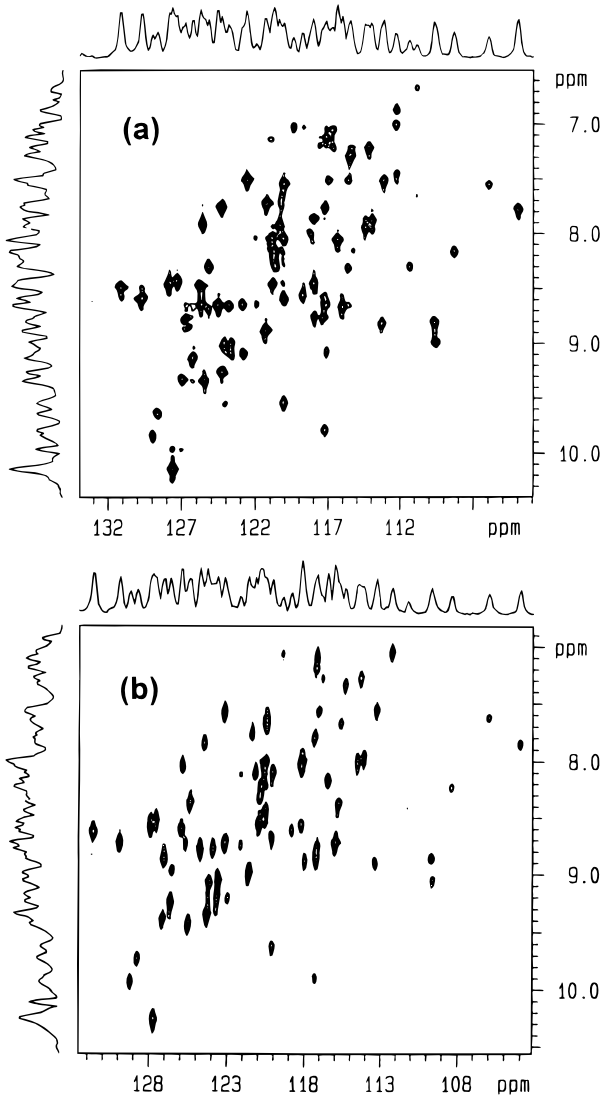

Figure 5. 2D ^{15}N–^{1}H chemical shift correlation NMR spectra of Pdx-^{15}N measured by the direct method at 40.55 MHz and 290 K, with ^{1}H decoupling in both dimensions, except for geminal ^{1}H–^{1}H couplings of $^{15}NH_2$ groups in the F_1 dimension: (a) HETCOR; (b) DEPT90 HETCOR (^{15}NH subspectrum).

However, the latter assumption appears to be true for only a certain range of distances (*ca.* 4–7 Å), in which other relaxation mechanisms (e.g. the contact mechanism due to electron delocalization) are negligible. Unpaired electron spin in the iron–sulfur cluster is assumed on average[17] to be localized between the two iron atoms, and the distances d_1 and d_2 between the nucleus and each of the two iron atoms are converted to the reduced distance d_r by means of the equation

$$d_r = \sqrt[6]{\frac{{d_1}^6 {d_2}^6}{{d_1}^6 + {d_2}^6}} \tag{3}$$

It has been pointed out[47] that the so called 'diamagnetism' of the oxidized 2Fe–2S proteins results from antiferromagnetic coupling of two ferric ions of spin $S_a = S_b = 5/2$ to a ground state of spin $S = 0$. However, the observed paramagnetic properties of the putidaredoxins must originate from a distribution of populations in higher spin states; for example, the first excited state with spin $S = 1$ occurs at an energy J above the ground state.[48] The quantity J/k, where k is the Boltzmann constant, has been estimated to be larger than 60 K from magnetic susceptibility measurements on oxidized putidaredoxin.[49] Other studies of diferric–disulfur proteins[50] have indicated that there is a ladder of spin states available to the coupled system that increments from $S_a + S_b = 10 \times \frac{1}{2} = 5$ (corresponding to 10 unpaired electron spins) to $S_a - S_b = 0$ in one spin-unit steps. The completely antiferromagnetic state $S_a - S_b = 0$ has the lowest energy, and the other spin states are expected to be increasingly populated at higher temperatures.[50]

Computation of distances d_r from the spin–lattice relaxation rate by means of Eqn (2) or its equivalent requires (a) that a weighted average spin quantum number be calculated from the populations of the various spin states and (b) a value for the correlation

Table 1. ^{15}N chemical shifts (δ_N) and T_1 values of selected residues[a] of Pdx-^{15}N grouped together by residue type

Residue	δ_N (ppm)	^{15}N T_1[b] of backbone ^{15}NH	σ[c] (s)
Y5	124.2	0.43	0.04
V6	128.9	0.35	0.04
V52	126.7	0.42	0.01
V74	114.4	0.42	0.03
G10	108.5	0.33	0.03
G31	106.1	0.36	0.10
G69	104.1	0.34	0.04
L15	125.7	0.37	0.06
L78	130.0	0.37	0.01
S29	114.2	0.42	0.02
N53	127.6	0.37	0.04
A18	131.7	0.34	0.03
A63	124.8	0.44	0.04
A76	124.5	0.42	0.04
E54	124.4	0.42	0.03
E72	112.4	0.35	0.04
E77	116.6	0.46	0.05
K79	129.3	0.35	0.04
C73	114.6	0.43	0.02
T75	111.3	0.37	0.03
T91	115.4	0.40	0.02
M90	125.2	0.41	0.01
W106	125.9	0.38	0.07
		T_1[b] (s) of other ^{15}N nuclei	
(K2, K59, K79)[d] $N_\zeta H_2$	31.8	1.73	0.05
	32.7	1.81	0.11
	33.6	0.32	0.11
(R12, R13, R66, R83, R104)[d] $N_\varepsilon H$	83.5	0.52	0.07
	84.3	0.81	0.13
	84.8	0.45	0.09
(R12, R13, R66, R83, R104)[d] $N_\eta H_2$	69.2	0.19	0.01
	69.4	0.21	0.02
	70.9	0.44	0.17
	71.1	0.43	0.13
N53 $N_\delta H_2$	115.7	0.41	0.02
N64 $N_\delta H_2$	110.8	0.27	0.02
N81 $N_\delta H_2$	111.9	0.25	0.03
(P61, P80, P92, P102)[d] N_α	133.8	1.69	0.21
	135.3	1.83	0.20
	137.5	1.68	0.18
	140.9	2.02	0.21
Q105 $N_\varepsilon H_2$	112.8	0.38	0.04
W106 $N_{\varepsilon 1} H$	127.8	0.38	0.03

[a] Resolved resonances in the 1D ^{15}N NMR spectrum.
[b] Mean value of mostly six measurements, except for occasional reduction to three to five measurements because of rejection of outliers.
[c] Standard deviation of the mean.
[d] Assignments are not specific.

time τ_c. For a temperature of 290 K, we used the parameters $kT = 201.6\ cm^{-1}$, $J = 200\ cm^{-1}$,[3,51] and[51] $C_i = \frac{1}{2}$ to calculate the expectation value $\langle S_z \rangle$ of S_z from the equation

$$\langle S_z \rangle = \frac{\sum_i C_i S_i(S_i+1)(2S_i+1)\exp(-E_{S_i}/kT)}{\sum_i (2S_i+1)\exp(-E_{S_i}/kT)} \quad (4)$$

thus taking into account the populations of spin states $S_i = 0$, 1, 2, 3, 4 and 5, having energies $E_{S_i} = 0$, J, $3J$, $6J$, $10J$ and $15J$, respectively.[10,51] The weighted average spin number for the Fe_2S_2 cluster may be taken[52] as the expectation value $\langle S_z \rangle$, for which Eqn (4), when calculated over both iron atoms, yielded a value of 1.67.

For most paramagnetic proteins, the correlation time τ_c is dominated[10] by the electron relaxation time τ_s (the fastest process). A good value of τ_s is not readily available for Pdx,[3] but based on literature values[10,13] for other ferredoxins, a likely value would be in the range 10^{-10}–10^{-11} s, although values as large as 10^{-9} s are possible.[52] In the fast motion limit[10] ($\tau_c \ll \omega_s^{-1}$, ω_I^{-1}), Eqn (2) can be reformulated as

$$T_1^{-1} = \frac{4}{3}\left(\frac{\mu_0}{4\pi}\right)^2 \frac{\gamma_N{}^2 g_e{}^2 \mu_B{}^2}{d_r{}^6} \times \frac{\sum_i C_i{}^2 S_i(S_i+1)(2S_i+1)\exp(-E_{S_i}/kT)}{\sum_i (2S_i+1)\exp(-E_{S_i}/kT)} \tau_c \quad (5)$$

We used Eqn (5) to calculate sets of reduced distances from the ^{15}N relaxation rates for the correlation time values $\tau_c = 10^{-10}$ and 10^{-11} s (Table 2).

Calculations of the spin of the iron–sulfur cluster and assumptions about the correlation time are avoided in a recently developed method in which a simplified form of Eqn (2):

$$\frac{1}{T_1} \times 10^2 = \frac{a}{d_r{}^6} \times 10^4 + b \quad (6)$$

is used.[20] For *Anabaena* 7120 heterocyst ferredoxin, the ^{15}N T_1 data were evaluated by fitting to this equation, where a and b are adjustable parameters, T_1 is the relaxation time in milliseconds and d_r the reduced distance in

Table 2. Reduced distances (d_r) of ^{15}N nuclei from the center of the iron–sulfur cluster of Pdx-^{15}N calculated from the ^{15}N T_1 values of resonances with ^{15}N chemical shifts δ_N for two correlation times τ_c

δ_N(ppm)	T_1[a] (ms)	σ[b] (ms)	d_r[c] (Å) $\tau_c = 10^{-10}$ s	$\tau_c = 10^{-11}$ s
106.6	33	13	4.1	2.8
108.8	138	12	5.2	3.5
114.4 (V74)	420	30	6.2	4.3
114.6 (C73)	430	20	6.2	4.3
124.8 (A63)	440	40	6.3	4.3
128.4	139	11	5.2	3.5
129.6	163	10	5.3	3.6
130.9	47	4	4.3	3.0
134.8	78	5	4.7	3.2
136.1	28	5	4.0	2.7
138.4	60	8	4.5	3.1
143.9	—[d]	—	—	—
145.8	46	4	4.3	2.9
149.1	68	8	4.6	3.1
150.8	50	2	4.4	3.0
155.4	24	1	3.9	2.6
157.5	35	1	4.1	2.8
181.8	—[d]	—	—	—
203.3	—[d]	—	—	—

[a] Mean value of mostly six determinations, except for occasional reduction to three to five determinations because of rejection of outliers.
[b] Standard deviation of the mean.
[c] Calculated by use of Eqn (5). A 10% deviation in T_1 value leads to a 1.5% change in the d_r value.
[d] Signal-to-noise ratio too low for measurement of T_1.

Å, the values of which were calculated from x-ray crystal structure data. The values $a = 2.170$ and $b = 0.1$ s^{-1} gave the best overall fit to the data, and the importance of testing this model on ^{15}N relaxation results from other paramagnetic proteins was stated.[20]

Our calculations using Eqn (6) with Chae and Markley's values[20] of a and b yielded reduced distances (see column 2 in Table 3) that are 0.3–0.6 Å larger than the values (column 1 in Table 3) that were calculated from Eqn (5) by using a weighted average spin of 1.67 for the iron–sulfur cluster and $\tau_c = 10^{-10}$ s. Both sets of reduced distances are of the same order as the numerically ordered reduced distances derived from the ^1H NMR structure[5] of Pdx. Agreement between the reduced distances calculated by use of Chae and Markley's parameters a and b with Eqn (6) and the distances calculated from the ^1H NMR structure of Pdx may be expected on the basis that this structure and the parameters a and b were at least partially derived by way of the same *Anabaena* ferredoxin model. However, the reduced distances calculated directly from Eqn (5) offer a more independent confirmation of the approximate magnitude of these distances, because this equation does not depend on the modeling of any particular protein, and has been used with an independent calculation of the spin number of the iron–sulfur cluster.

Clearly, the oxidized ferredoxin from *Anabaena* 7120 is a good model for Pdx because of the high degree of structural homology in certain regions of these proteins and the similarity around their iron–sulfur clusters.[6] According to ^{15}N T_1 data for the ferredoxin, the C41, C46, C49 and C79 residues are bound to the two iron atoms with reduced distance values[20] in the range of 3.5–4.1 Å. Likewise, the average NMR structure of Pdx indicates that its residues C39, C45, C48 and C86 have reduced distance values in the range 3.9–5.1 Å. However, this difference may be influenced by the fact that the NMR structure of Pdx was obtained by an overall energy minimization of the protein, rather than from NOE constraints for the paramagnetic region, that are not readily available.

Table 3. Comparison of reduced distances (d_r) of ^{15}N nuclei in various residues from the center of the iron–sulfur cluster of Pdx-^{15}N with those computed from the published structure of Pdx determined by ^1H NMR and structural analogy with *Anabaena* ferredoxin

d_r (Å) from ^{15}N T_1 values[a]		d_r (Å) from ^1H	
From Eqn (5)[b]	From Eqn (6)[c]	NMR structure	Residue
3.9	4.2	3.9	C39
4.0	4.3	4.0	C45
4.1	4.4	4.5	C86
4.1	4.5	4.6	G40
4.3	4.7	4.7	S44
4.3	4.7	5.1	C85
4.4	4.7	5.1	C48
4.5	4.9	5.1	D38
4.6	5.0	5.2	A46
4.7	5.1	5.4	A43
5.2	5.7	5.6	T47
5.2	5.7	5.9	Q87
5.3	5.9	6.2	G41
		6.3	L84
		6.4	S42

[a] The d_r values calculated from the ^{15}N T_1 values are not assigned to specific residues, but are merely ranked and listed according to their apparent agreement with the d_r values computed from the ^1H NMR structure of Pdx.
[b] Calculated by using $\tau_c = 10^{-10}$ s.
[c] Calculated by use of the parameters[20] $a = 2.170$ and $b = 0.1$ s^{-1}.

CONCLUSIONS

We detected 16 paramagnetically broadened ^{15}N NMR resonances for Pdx-^{15}N by direct observation of 1D ^{15}N NMR spectra at 40.55 MHz. Also detected were four sharp ^{15}N resonances for the proline residues, three lysine side-chain ^{15}N resonances and several other side-chain ^{15}N resonances. None of the aforementioned ^{15}N resonances has been detected previously by ^1H detected ^{15}N NMR studies, since the ^1H NMR signals of amino acid residues that are close to the iron–sulfur cluster of Pdx are insufficiently intense or well resolved to allow ^1H–^{15}N connectivities to be established. Because most of the residues that are missing from the ^1H detected data reported previously are amino acid residues without side-chain nitrogen atoms, we can conclude that the majority of our 16 broad ^{15}N resonances originate from the backbone ^{15}N atoms of residues that are close to the paramagnetic center. By use of directly observed ^{15}N NMR spectra and the inversion–recovery method, we measured a set of ^{15}N spin–lattice relaxation times (T_1) from those resonances that are clearly separated and/or are sufficiently intense in the 1D ^{15}N NMR spectra, including data from a number of broadened and unbroadened signals that originate from backbone ^{15}N atoms both within and without the paramagnetic zone of the protein, respectively. By analysis of the ^{15}N T_1 values, we calculated reduced distances of ^{15}N nuclei from the iron–sulfur cluster for a number of such nuclei that are within *ca.* 4–7 Å of this cluster, this being the valid range of distances for calculations based on the assumption of relaxation by a dominant electron → nuclear dipole–dipole interaction. Ranked by size, the resulting reduced distances are in reasonable agreement with the range of distances calculated as averages (Table 3) of the distances in 12 closely related structures of Pdx that have been defined by homonuclear ^1H NMR methods in combination with a model based on a related *Anabaena* ferredoxin.[6] For paramagnetic proteins that do not readily exhibit ^1H–^1H NOEs within the paramagnetic zone, the present results emphasize the utility of the determination of distances within this zone from ^{15}N T_1 data. ^{15}N linewidth or transverse relaxation time (T_2) measurements could be considered as alternative methods for the purpose of obtaining structural information around the paramagnetic center.

Acknowledgements

Thanks are due Dr Soojay Banerjee for helpful discussions, Dr David Bunk for mass spectra, Mr M. P. Mayhew for technical help, Dr John Orban for access to a Bruker AMX-500 NMR spectrometer, Dr T. C. Pochapsky for supplying digital copies of NMR data and Dr A. E. Roitberg for numerical calculations.

REFERENCES

1. D. W. Cushman, R. L. Tsai and I. C. Gunsalus, *Biochem. Biophys. Res. Commun.* **26**, 577 (1967).
2. T. C. Pochapsky, T. A. Lyons, S. Kazanis, T. Arakaki and G. Ratnaswamy, *Biochimie* **78**, 723 (1996).
3. G. Ratnaswamy and T. C. Pochapsky, *Magn. Reson. Chem.* **31**, S73 (1993).
4. T. C. Pochapsky and X. M. Ye, *Biochemistry* **30**, 3850 (1991).
5. X. M. Ye, T. C. Pochapsky and S. S. Pochapsky, *Biochemistry* **31**, 1961 (1992).
6. T. C. Pochapsky, X. M. Ye, T. Ratnaswamy and T. A. Lyons, *Biochemistry* **33**, 6424 (1994).
7. T. C. Pochapksy, G. Ratnaswamy and A. Patera, *Biochemistry* **33**, 6433 (1994).
8. S. Kazanis, T. C. Pochapsky, T. M. Barnhart, J. E. Penner-Hahn, U. A. Mirza and B. T. Chait, *J. Am. Chem. Soc.* **117**, 6625 (1995).
9. T. A. Lyons, G. Ratnaswamy and T. C. Pochapsky, *Protein Sci.* **5**, 627 (1996).
10. I. Bertini and C. Luchinat, in *NMR of Paramagnetic Molecules in Biological Systems*, edited by A. B. P. Lever and H. B. Gray. pp. 50–221. Benjamin/Cummings, Menlo Park, CA (1986).
11. I. Bertini, L. Banci and C. Luchinat, *Methods Enzymol.* **177**, 246 (1989).
12. I. Bertini, F. Briganti, C. Luchinat, A. Scozzafava and M. Sola, *J. Am. Chem. Soc.* **113**, 1237 (1991).
13. I. Bertini, P. Turano and A. J. Vila, *Chem. Rev.* **93**, 2833 (1993).
14. E. Lebrun, C. Simenel, F. Guerlesquin and M. Delepierre, *Magn. Reson. Chem.* **34**, 873 (1996).
15. W. R. Rypniewski, D. R. Breiter, M. M. Benning, G. Wesenberg, B.-H. Oh, J. L. Markley, I. Rayment and H. M. Holden, *Biochemistry* **30**, 4126 (1991).
16. G. W. Canters, C. W. Hilbers, M. Van de Camp and S. S. Wijmenga, *Methods Enzymol.* **227**, 244 (1993).
17. B.-H. Oh and J. L. Markley, *Biochemistry* **29**, 4012 (1990).
18. B.-H. Oh, E. S. Mooberry and J. L. Markley, *Biochemistry* **29**, 4004 (1990).
19. H. Cheng, B. Xia, Y. K. Chae, W. M. Westler and J. L. Markley, in *Proceedings of the Conference on Stable Isotope Applications in Biomolecular Structure and Mechanisms*, edited by J. Trewhella, T. A. Cross and C. J. Unkefer. p. 171. Los Alamos National Laboratory, Los Alamos, NM (1994).
20. Y. K. Chae and J. L. Markley, *Biochemistry* **34**, 188 (1995).
21. P. Reddy, A. Peterkofsky and K. McKenney, *Nucleic Acids Res.* **17**, 10473 (1989).
22. H.-U. Bernard and D. R. Helinski, *Methods Enzymol.* **68**, 482 (1979).
23. J. Sambrook, E. F. Frisch and T. Maniatis, *Molecular Cloning—a Laboratory Manual*. p. A2. Cold Spring Harbor Laboratory Press, Plainview, NY (1989).
24. D. A. Grayson, Y. B. Tewari, M. P. Mayhew, V. L. Vilker and R. N. Goldberg, *Arch. Biochem. Biophys.* **332**, 239 (1996).
25. D. Marion and K. Wüthrich, *Biochem. Biophys. Res. Commun.* **113**, 967 (1983).
26. A. Wokaun and R. R. Ernst, *Chem. Phys. Lett.* **52**, 407 (1977).
27. M. Rance, O. W. Sorensen, G. Bodenhausen, G. Wagner, R. R. Ernst and K. Wüthrich, *Biochem. Biophys. Res. Commun.* **117**, 479 (1983).
28. A. E. Derome and M. P. Williamson, *J. Magn. Reson.* **88**, 177 (1990).
29. J. Jeener, B. H. Meier, P. Bachmann and R. R. Ernst, *J. Chem. Phys.* **71**, 4546 (1979).
30. G. Bodenhausen, H. Kogler and R. R. Ernst, *J. Magn. Reson.* **58**, 370 (1984).
31. A. A. Bothner-By, R. L. Stephens, J. M. Lee, C. D. Warren and R. W. Jeanloz, *J. Am. Chem. Soc.* **106**, 811 (1984).
32. A. Bax and D. G. Davis, *J. Magn. Reson.* **63**, 207 (1985).
33. L. Braunschweiler and R. R. Ernst, *J. Magn. Reson.* **53**, 521 (1983).
34. A. Bax and D. G. Davis, *J. Magn. Reson.* **65**, 355 (1985).
35. G. Bodenhausen and D. J. Ruben, *Chem. Phys. Lett.* **69**, 185 (1980).
36. A. Bax and S. Subramanian, *J. Magn. Reson.* **67**, 565 (1986).
37. A. J. Shaka, P. B. Barker and R. Freeman, *J. Magn. Reson.* **64**, 547 (1985).
38. A. J. Shaka, J. Keeler, T. Frenkiel and R. Freeman, *J. Magn. Reson.* **52**, 335 (1983).
39. D. M. Doddrell, D. T. Pegg and M. R. Bendall, *J. Magn. Reson.* **48**, 323 (1982).
40. B. Coxon, *J. Magn. Reson.* **66**, 230 (1986).
41. B. Coxon, *Magn. Reson. Chem.* **24**, 1008 (1986).
42. R. L. Vold, J. S. Waugh, M. P. Klein and D. E. Phelps, *J. Chem. Phys.* **48**, 3831 (1968).
43. A. Bax, *J. Magn. Reson.* **53**, 517 (1983).
44. B. Coxon, *Magn. Reson. Chem.* **26**, 449 (1988).
45. B. Coxon, *Can. J. Chem.* **68**, 1145 (1990).
46. B. Coxon, in *NMR Applications in Biopolymers*, edited by J. W. Finley, S. J. Schmidt and A. S. Serianni. p. 27. Plenum Press, New York, (1990).
47. J. F. Gibson, D. O. Hall, J. H. M. Thornley and F. R. Whatley, *Proc. Natl. Acad. Sci. USA* **56**, 987 (1966).
48. E. Münck, P. G. Debrunner, J. C. M. Tsibris and I. C. Gunsalus, *Biochemistry* **11**, 855 (1972).
49. C. Moleski, T. H. Moss, W. H. Orme-Johnson and J. C. M. Tsibris, *Biochim. Biophys. Acta* **214**, 548 (1970).
50. G. Palmer, in *Iron–Sulfur Proteins, Molecular Properties*, Vol. 2, edited by W. Lovenberg. p. 285. Academic Press, New York (1973).
51. L. Banci, I. Bertini and C. Luchinat, *Struct. Bonding* **72**, 113 (1990).
52. I. Bertini and C. Luchinat, in *Coordination Chemistry Reviews 150: NMR of Paramagnetic Substances*, edited by A. B. P. Lever. pp. 1–161. Elsevier, Amsterdam (1996).

